J Neuropathol Exp Neurol
Vol. 79, No. 6, June 2020, pp. 585–591
doi: 10.1093/jnen/nlaa029

ORIGINAL ARTICLE

Distribution of TDP-43 Pathology in Hippocampal Synaptic Relays Suggests Transsynaptic Propagation in Frontotemporal Lobar Degeneration

Pouya Jamshidi, MD, Garam Kim, MS, Ryan K. Shahidehpour, MA, Kabriya Bolbolan, BS, Tamar Gefen, PhD, Eileen H. Bigio, MD, Marek-Marsel Mesulam, MD, and Changiz Geula, PhD

Abstract

Hyperphosphorylation, nuclear depletion, and aggregation of TDP-43 in ubiquitinated inclusions is a hallmark of frontotemporal lobar degeneration (FTLD-TDP). Evidence of potential spread of TDP-43 along synaptic connections in the human is largely limited to qualitative and semiquantitative observations. We quantitatively investigated potential transsynaptic propagation of TDP-43 across the well-established chain of single synaptic connections of the hippocampus. Hippocampi from 5 participants with clinical diagnoses of primary progressive aphasia and 2 participants with behavioral variant frontotemporal dementia, all with postmortem diagnoses of FTLD-TDP, were examined. TDP-43-positive mature (darkly stained) and pre-inclusions (diffuse puncta or fibrillar staining) in the granule cell layer of dentate gyrus (DG) and pyramidal cell layers of Cornu Ammonis (CA)3, CA2, and CA1 were quantified using unbiased stereology. The density of mature TDP-43 inclusions was higher in the DG than in the CA fields ($p < 0.05$). There were no differences in inclusion densities across the CA fields. TDP-43 pre-inclusions densities were not different across the 4 subregions. There was significantly higher preinclusion density than mature inclusions in CA3, but not in other subregions. Analysis of normalized total counts in place of densities revealed virtually identical results. Our finding of greatest mature inclusion deposition in the DG, coupled with more preinclusions than mature inclusions at the next relay station (CA3), and reduced densities of both in CA2-CA1, provide evidence in support of a sequential transsynaptic propagation mechanism of TDP-43 aggregates.

Key Words: Frontotemporal lobar degeneration (FTLD), Hippocampus, Primary progressive aphasia (PPA), Prion-like, TDP-43.

INTRODUCTION

Frontotemporal lobar degeneration (FTLD) is the second most common neuropathology underlying clinical dementia syndromes (1) and shares a similar prevalence to Alzheimer disease (AD) for individuals under the age of 65 (2). FTLD is known to cause several debilitating progressive syndromes, including a behavioral variant of frontotemporal dementia (bvFTD) with or without amyotrophic lateral sclerosis (ALS), and primary progressive aphasia (PPA) (3–6). Despite sharing a common underlying pathology, the clinical manifestations in these disorders are diverse. They include the behavioral and executive cognitive deficits of bvFTD with or without motor neuron dysfunction, and the language abnormalities of PPA (7–10). The heterogeneity of clinical presentations, distribution of neurodegeneration, and type of histopathologic markers contribute to the current difficulties in understanding the mechanisms of regional selectivity and patterns of disease progression.

A major form of FTLD is characterized pathologically by deposition of 43-kDa transactivation response element DNA-binding protein (TDP-43) inclusions and is designated FTLD-TDP (3, 11). The progressive aggregation and propagation of TDP-43 in the form of abnormal inclusions is similar to the accumulation of abnormal inclusions in other neurodegenerative diseases, such as AD and Parkinson disease (12). While the mode of propagation of these inclusions remains largely unknown, an exciting insight in the field has been the identification of disease spread through axonal pathways and prion-like mechanisms. Such transsynaptic propagation is not only a feature of prion proteins (13), but also has been described for phosphorylated tau in neurofibrillary tangles in animal models of AD (14, 15), and for α-synuclein in an animal model of Parkinson disease (16). Transsynaptic spread has also been implicated for TDP-43 in ALS (17), based on qualitative staging of appearance of TDP-43 inclusions (18). It has

From the Mesulam Center for Cognitive Neurology and Alzheimer's Disease, Feinberg School of Medicine, Northwestern University, Chicago, Illinois (PJ, GK, RKS, KB, TG, EHB, M-MM, CG).
Send correspondence to: Changiz Geula, PhD, Mesulam Center for Cognitive Neurology and Alzheimer's Disease, Feinberg School of Medicine, Northwestern University, 320 E. Superior Street, Searle 11-467, Chicago, IL 60611; E-mail: c-geula@northwestern.edu
Pouya Jamshidi and Garam Kim contributed equally to this work.
This study was supported by grants from the National Institute of Neurological Disorders and Stroke (NS085770), National Institute on Deafness and Other Communication Disorders (DC008552), the Jerome and Florane Rosenstone Fellowship, the Louis Family Foundation, an Alzheimer's Disease Center Grant from the National Institute on Aging (AG013854), and a training grant from the National Institute on Aging (T32 AG20506).
The authors have no duality or conflicts of interest to declare.

been demonstrated that TDP-43 contains a prion-like domain (19–21) and that seeding of aggregated TDP-43 in neurons results in formation of inclusions (17, 22, 23), supporting the possibility of transsynaptic propagation.

The aim of this study was to determine whether TDP-43 aggregates display characteristics of transsynaptic (prion-like) propagation along axonal projection pathways using a well-established neural circuit with multiple relays, in brains of 7 human subjects with postmortem pathologic diagnoses of FTLD-TDP. The hippocampus was selected for this investigation because it contains a serially arranged and highly ordered chain of intrinsic connections that link cytoarchitectonically distinct zones (24), and because dentate gyrus (DG) granule cells of the hippocampal formation are known to be vulnerable to TDP-43 inclusion formation (25, 26). The granule cells of the DG receive input from a variety of extrinsic sources, primarily through their dendritic trees in the molecular layer of the DG. These dentate granule cells then send a zinc-rich, dense "mossy fiber" projection to Cornu Ammonis (CA)3, where they synapse primarily on the dendritic spines of CA3 neurons. CA3 neurons, in turn, send collaterals of their extrinsically projecting axons ("Schaffer collaterals") to other portions of CA3 as well as to the pyramidal cells of CA2 and CA1 (24).

In addition to unbiased stereological quantitation of TDP-43 inclusions along this polysynaptic chain, the possibility of sequential formation and spread of pathologic TDP-43 was further investigated through quantification of TDP-43 "preinclusions," which potentially represent an earlier stage in the formation of a TDP-43 inclusion (27, 28). In a previous study, we found an inverse relationship between the densities of TDP-43 mature inclusions and preinclusions in FTLD-TDP (27). We also found that some cortical regions contain only preinclusions with a complete absence of mature inclusions, while the reverse was not seen, suggesting that mature inclusions are preceded by preinclusions. Thus, we postulated that the greatest density of mature inclusions would be seen at the "earliest" point of hippocampal connectivity (i.e. the granule cells of the DG, which are vulnerable to TDP-43 deposition [25, 26]), with decreasing density at later stations within the hippocampal circuitry (CA1–CA3). Conversely, we hypothesized that the CA fields, and particularly CA3, would contain a greater density of preinclusions when compared with inclusions, representing more recent arrival of TDP-43 pathology.

MATERIALS AND METHODS

Cohort, Tissue Preparation, and Pathologic Diagnoses

Five participants with a clinical diagnosis of PPA and two participants with bvFTD were included in this study. The diagnosis of PPA requires a clinical history of progressive language impairment unaccompanied by consequential decline in other cognitive domains within the initial stages of the disease (10, 34). A diagnosis of bvFTD is based on the 2011 work of the International Behavioral Variant FTD Consortium, which generated a set of sensitive and specific clinical criteria for diagnosing bvFTD (5). The seven participants were selected randomly from the separate available pools of PPA and bvFTLD cases which had either MRI or photographs of whole brain after autopsy, allowing determination of cortical atrophy. Four PPA participants were right-handed and had asymmetric left hemisphere atrophy, and one PPA participant was left-handed with asymmetric right hemisphere atrophy. One bvFTD participant was right-handed with right greater than left atrophy in the frontal lobe, and the other bvFTD participant was left-handed with no asymmetry in atrophy.

All tissue was obtained from the Northwestern University Alzheimer's Disease Center Brain Bank. Following autopsy, the cerebral hemispheres were separated in the midsagittal plane, cut into 2- to 3-cm coronal slabs, fixed in formalin or 4% paraformaldehyde, taken through sucrose gradients (10%–40%) for cryoprotection, and stored in 40% sucrose. Blocks of tissue were sectioned at 40-μm thickness and stored in 0.1 M phosphate buffer containing 0.2% sodium azide at 4°C until use. Pathological diagnosis of FTLD and specification of its variants was rendered by a neuropathologist using the published consensus criteria of the Consortium for FTLD (12). Of the 5 brains coming from PPA participants, 3 had FTLD-TDP Type A pathology and 2 had FTLD-TDP Type B pathology. The 2 bvFTD brains had diagnoses of FTLD-TDP Type A (participant 6) and Type B (participant 7) pathology. Brains displaying concomitant hippocampal sclerosis, which is seen in a proportion of FTLD cases, were excluded. Additional characteristics of the participants, such as sex, disease duration, age at death and postmortem interval, are presented in Table 1.

Immunohistochemistry

A 1 in 24 series of coronal sections was immunohistochemically stained using the avidin-biotin-peroxidase complex (ABC) method employing the Vectastain Elite ABC kit (Vector Laboratories, Burlingame, CA) as described previously (29, 30). An antibody against human phosphorylated TDP-43 (pSer409/410, Cosmo Bio, Tokyo, Japan; polyclonal) was used to visualize TDP-43-positive neuronal cytoplasmic inclusions (NCI), neuronal intranuclear inclusions (NII), dystrophic neurites (DN), and preinclusions.

Unbiased Stereological Quantitative Estimation

Total numbers of TDP-43 NCI, NII, DN, and preinclusions (diffuse cytoplasmic and occasionally nuclear staining [27]) in areas populated by neurons (granule cell layer of DG and pyramidal cell layers of CA3, CA2, and CA1) were estimated using unbiased stereological counting in the StereoInvestigator software (MicroBrightField, Inc., Williston, VT), as described previously (31). Briefly, regularly sampled series of sections through the areas of interest were analyzed using the optical fractionator method. The boundaries of each cortical area were delineated in stained sections at 4× magnification, and a 60× objective was used for quantification. Guard heights of 2 μm and a dissector height of 16 μm were used. The parameters, which were derived from pilot studies on a subsample of cases, resulted in coefficients of error (Gunderson, $m = 0$) of $<10\%$. All results were converted to counts per

TABLE 1. Characteristics of PPA (n = 5) and bvFTD (n = 2) Participants

Case	Clinical Diagnosis	Gender	FTLD-TDP Subtype	Race	Handedness	Age at Death	Brain wt (g)	Disease Duration (years)	PMI (hours)	Fixation Method
1	PPA-G	Male	Type A	C	Right	70	999	4	4	F
2	PPA-L	Male	Type A	C	Left	65	1040	8	6	F
3	PPA-M	Female	Type A	C	Right	74	1035	7	10	F
4	PPA-G	Male	Type B	C	Right	55	1090	4	29	F
5	PPA-L → PPA-G	Male	Type B	C	Right	59	1490	2	12	F
6	bvFTD	Female	Type A	C	Right	65	980	8	unk	P
7	bvFTD	Female	Type B	C	Left	59	810	8	23	F

PPA clinical subtypes: L, logopenic; G, agrammatic; M, mixed. Participant 5 progressed from logopenic to agrammatic. bvFTD, behavioral variant frontotemporal dementia. Race: C, Caucasian; PMI, postmortem interval; unk, unknown. Fixation method: F, formalin; P, 4% paraformaldehyde.

cubic millimeter using the planimetric volume estimated by the StereoInvestigator software. To account for differences in the size of each region, we also used normalized total counts for analysis. Counts were normalized to adjust for the number of sections used for stereological quantitation in each region.

Statistical Analysis

All data analyses were performed using SAS 9.4 software (version 5.03; SAS Institute Inc., Cary, NC). A mixed-model repeated measures analysis of variance (RM-ANOVA) was used to compare inclusion densities and normalized total counts across each synaptic relay starting in the DG and ending in CA2-CA1 sectors, accounting for subject-specific random effects. RM-ANOVA tests were conducted separately for TDP-43 mature and preinclusions, and additionally to assess the relationship between the two inclusion types. Wilcoxon ranked sum tests were used to test for differences between the two clinical subgroups. Paired *t*-tests were used to assess asymmetry of pathologic deposition across the language-dominant and nonlanguage-dominant hemispheres in PPA cases. All tests were two-tailed, and p-values <0.05 were considered significant.

RESULTS

Distribution of Hippocampal TDP-43 Mature Inclusions in FTLD-TDP

We analyzed the distribution patterns of mature TDP-43 inclusions in brains of individuals who had clinically presented with PPA or bvFTD (Table 1). These cases were a mixture of FTLD-TDP Type A (n = 4) and B (n = 3).

Across all participants, the highest numbers of TDP-43 inclusions were found in the granule neurons of the DG in each hemisphere, with significantly fewer inclusions in pyramidal neurons of CA3 (one synaptic relay away) ($p = 0.0174$), CA2 ($p = 0.0181$), and CA1 ($p = 0.0187$) (Figs. 1A, B and 2A). However, there were no significant differences in TDP-43 inclusion densities between the three CA fields ($p > 0.05$). Our qualitative observations revealed no differences in the pattern of TDP-43 inclusions and preinclusions when comparing PPA and bvFTD cases or FTLD-TDP Type A and Type B cases. Statistically, no significant differences were noted between FTLD-TDP Type A and Type B cases ($p > 0.05$). The low number of bvFTD participants (n = 2) did not allow proper statistical analysis of bvFTD versus PPA.

Distribution Patterns of Preinclusions in Hippocampal Circuits: Quantitative and Qualitative Observations

Two main types of preinclusions were observed throughout the cases—a granular type and a fibrillar type; however, the overwhelming majority of preinclusions was of the granular cytoplasmic type. Thus, for the purpose of analysis, the preinclusion types were combined. Unlike mature inclusions, preinclusion densities were not statistically significantly different across the four hippocampal subregions (Fig. 2B). However, two distinct patterns emerged qualitatively on a case-by-case basis.

In pattern I, the highest density of preinclusions was found in the DG, followed by a slightly lesser density in the CA3, and even less in CA2 and CA1 (i.e. in the shape of a quadratic growth curve) (cases 1, 2, and 4) (Fig. 1). In pattern II, there was zero to little density of preinclusions in the DG, followed by a spike in density in the CA3, then either similar or lesser densities (compared with CA3) in the CA2 and CA1 (cases 3, 5, 6, and 7).

No Asymmetry of Hippocampal TDP-43 Pathology in PPA or bvFTD

Since PPA is a highly asymmetric syndrome—in that the prominence of language symptoms is often associated with a distinct pattern of asymmetric and focal atrophy (32) and TDP-43 inclusions favor language regions asymmetrically (30, 33)—we assessed differences across the language-dominant and nonlanguage-dominant hemispheres within the five PPA cases. Paired *t*-tests revealed no significant differences in mature inclusion counts across the hemispheres ($p > 0.05$) (Fig. 2A). Given that the hippocampus is spared in PPA (a clinical syndrome with predominantly language deficits), this lack of asymmetry was not surprising. Similarly, no significant asymmetry was present in preinclusion counts ($p > 0.05$) (Fig. 2B). Additionally, qualitative observations indicated no asymmetries in the densities of mature or preinclusions in the bvFTD participants.

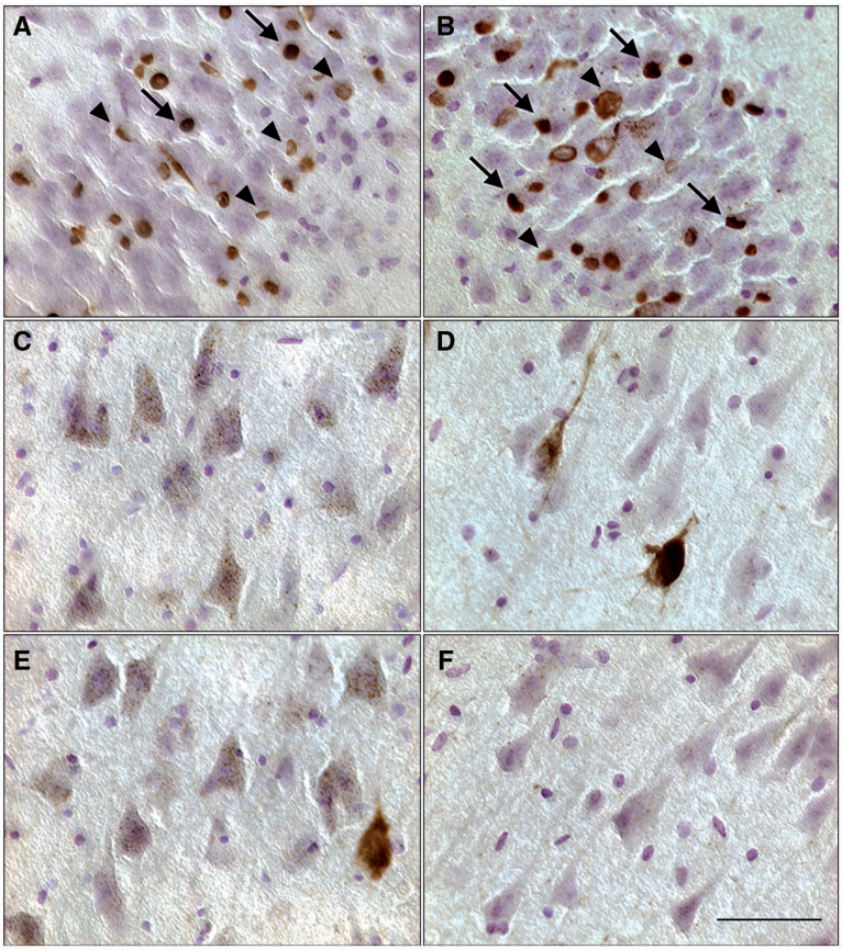

FIGURE 1. Distribution of mature and preinclusions in the hippocampus. **(A, B)** Granule cells of the dentate gyrus display high densities of both TDP-43 mature inclusions (arrows) and preinclusions (arrowheads). **(C, D)** Pyramidal cells in the CA3 field of the hippocampus show high density of preinclusions while demonstrating a near absence of mature inclusions. **(E, F)** CA1 region displays considerably fewer preinclusions, and in some fields **(E)**, no preinclusions. Mature inclusions were virtually absent from the CA1 field of the hippocampus. Occasionally, sparsely populated preinclusions in the CA fields displayed more intense staining **(D, F)**. Scale bar = 50 μm.

Relationship Between TDP-43 Mature and Preinclusions

Based on lack of hemispheric asymmetry, counts from the language-dominant and nonlanguage-dominant hemispheres were combined to assess significant differences in TDP-43 mature versus preinclusion densities. Unlike the DG, CA1, and CA2, which displayed no significant differences when mature and preinclusion densities were compared, CA3 had significantly higher densities of preinclusions than mature inclusions ($p = 0.0054$) (Fig. 3). It is worth noting that while there was overlap between the number of inclusions and preinclusions in the DG, there was distinctly no overlap in any of the CA fields (Fig. 3).

Analysis of Normalized Total Counts

Measures of density used in our study may be subject to variation due to differential atrophy of various regions investigated in FTLD-TDP. To address this issue, we also conducted analyses using total counts of TDP inclusions and preinclusions. To further control for the size of the area investigated, all counts were normalized to the area that spanned the least number of sections. Results obtained after analysis of normalized total counts were nearly identical to the results obtained using the density of inclusions and preinclusions (Table 2). No asymmetry was observed across the language-dominant versus nonlanguage-dominant hemispheres ($p > 0.05$); therefore, data were combined across hemispheres for the remainder of this analysis. The DG granule cells contained significantly larger numbers of TDP-43 inclusions when compared with all CA fields ($p < 0.0003$) (Fig. 4). However, the density of preinclusions did not display statistically significant differences among hippocampal subfields ($p > 0.05$), due to higher numbers of preinclusions when compared with mature inclusions in the CA fields, particularly CA3 (Fig. 4).

DISCUSSION

A growing body of evidence at both the biochemical and histopathological level suggests that TDP-43 propagates

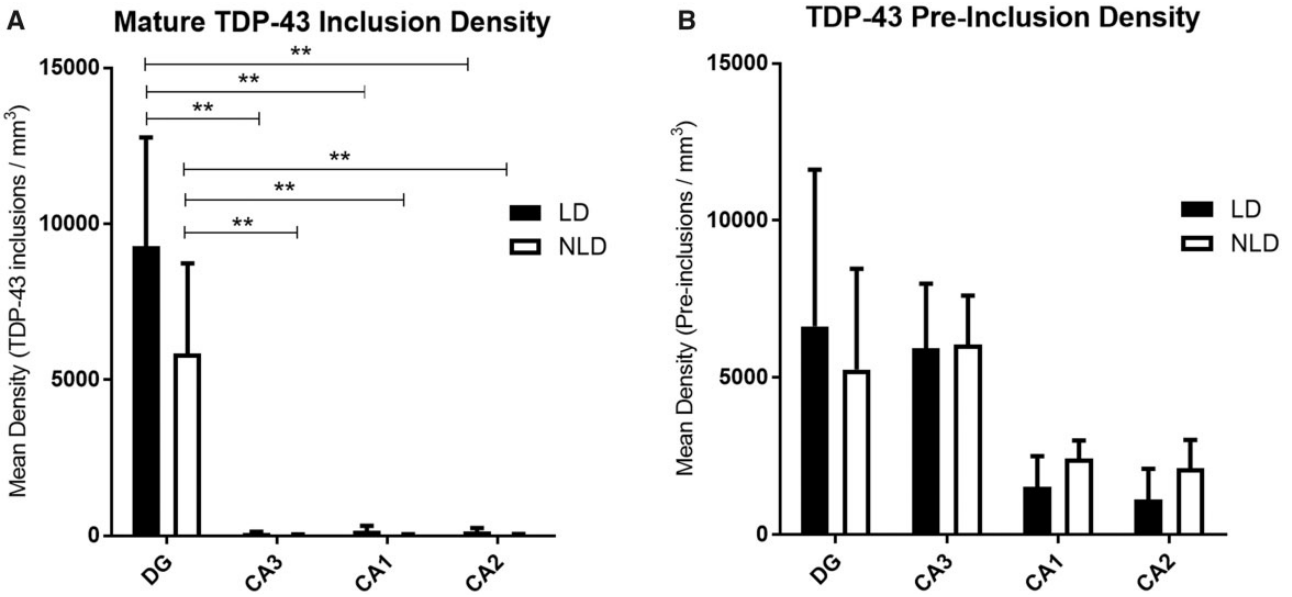

FIGURE 2. Bar graphs of TDP-43 mature inclusion **(A)** and preinclusion **(B)** densities when all cases were combined. Mature inclusions were significantly more abundant in the dentate gyrus than in CA3, CA2, and CA1. Note that there is no significant asymmetry between the language-dominant and nonlanguage-dominant hemispheres for mature or preinclusions within any of the hippocampal subregions. DG, dentate gyrus; CA, Cornu Ammonis; LD, language-dominant hemisphere; NLD, nonlanguage-dominant hemisphere; ** $p < 0.05$.

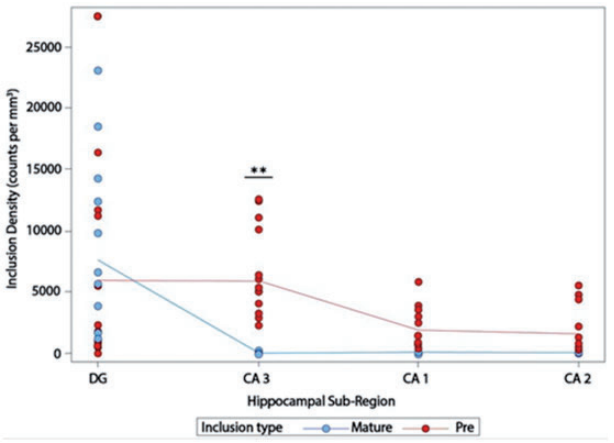

FIGURE 3. Densities of TDP-43 mature and preinclusions across the four hippocampal subregions and both hemispheres. Note the significant difference in pre- and mature-inclusion densities in CA3 and lack of overlap between mature inclusions and preinclusions in the CA fields. DG, dentate gyrus; CA, Cornu Ammonis; **$p < 0.01$.

through a seeding or prion-like mechanism and likely acts through axonal pathways (18–23). While the precise neurobiological and molecular mechanisms and directionality of pathologic TDP-43 spread are yet to be elucidated, it is recognized that changes in physiological TDP-43 function may result from a loss-of-function due to mislocalization or complications in TDP-43 clearance from the nucleus, or from a toxic gain-of-function caused by abnormal cleavage, hyperphosphorylation, and aggregation (19).

To assess a potential transsynaptic and sequential distribution of TDP-43 inclusions, we applied a stereological quantitative approach based on the presumption that inclusions would develop consecutively at hippocampal relay stations. Under this theoretical mode of pathologic spread, we postulated that the greatest dysfunction (i.e. mature inclusion deposition) would be seen at the "earliest" point of connectivity, with decreasing severity at later stations within the hippocampal circuitry. Previous studies had already shown that the granule cells of the DG are vulnerable to TDP-43 deposition (25, 26). Consistent with our hypothesis, the highest deposition of mature TDP-43 inclusions was at the earliest relay station in the hippocampal circuit—the DG—followed by progressively and substantially lesser densities in the three connected CA fields, supporting the concept that TDP-43 is aggregating in a sequential and orderly manner.

Our finding of a significantly higher density of preinclusions than mature inclusions in the CA3 field, coupled with the two patterns we qualitatively describe of the diffuse, earlier-stage TDP-43 preinclusions (highest density of preinclusions either in the DG or in the CA3 region), further supports the hypothesis of sequential formation and spread. Based on our earlier studies suggesting that preinclusions precede the formation of mature inclusions (i.e. the region with highest number of preinclusions would be the region with most recent pathology), our quantitative and qualitative observations of highest preinclusion density in CA3 or DG is supportive of the transsynaptic model of propagation. A more detailed study with a larger cohort and mechanistic confirmation at the molecular level in animal models is necessary to corroborate these conclusions.

TABLE 2. Normalized Counts of TDP-43 Inclusions and Preinclusions in Hippocampal Sectors of Each Hemisphere in Each Case

Case	Inclusions								Preinclusions							
	DG		CA3		CA1		CA2		DG		CA3		CA1		CA2	
	Left	Right	Left	Right	Left	Right	Left	Right	Left	Right	Left	Right	Left	Right	Left	Right
1	13 761	3274	5213	0	32 479	370	7175	0	31 340	92 266	61 250	84 891	16 876	43 933	2448	7017
2	4503	7130	185	883	0	0	128	0	69 236	65 358	102 813	67 933	66 503	19 320	7051	1815
3	48 298	15 601	3881	536	1511	501	406	0	17 384	5200	143 206	173 544	29 846	121 230	6086	14 168
4	178 398	130 474	2133	1547	3807	5861	1046	2096	212 680	5305	190 887	144 724	177 124	164 102	48 878	53 962
5	77 221	38 430	277	355	356	0	0	0	78	0	58 119	116 971	80 003	209 302	10 771	39 351
6	38 778	22 282	222	1109	0	335	150	137	6138	10 695	107 207	84 977	14 563	25 832	1947	5907
7	46 369	30 656	761	1129	0	0	0	0	1840	17 224	186 053	203 758	29 294	70 797	7267	15 691

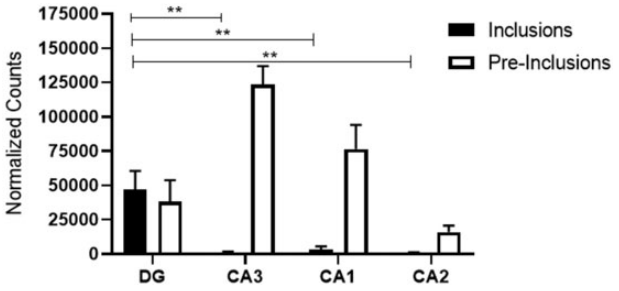

FIGURE 4. Normalized total counts of TDP-43 inclusions and preinclusions in hippocampal sectors. The number of inclusions in the dentate gyrus was significantly higher than in CA fields. The density of preinclusions showed no significant differences among hippocampal sectors. Note the presence of large number of preinclusions when compared with inclusions in CA3. DG, dentate gyrus; CA, Cornu Ammonis; **$p < 0.0003$.

Thus, the current study provides evidence for a sequential, transsynaptic propagation of TDP-43 pathology through the intrinsic hippocampal circuitry. Moreover, our data indicate that the mechanism of TDP-43 propagation in FTLD may be similar in bvFTD and PPA, which are two highly distinct clinical dementia syndromes. Considering that the hippocampus is relatively preserved in both clinical syndromes, in terms of atrophy and symptomatic presentation, this lack of difference is not surprising.

We also investigated hemispheric asymmetry of TDP-43 pathology in cases that had presented with PPA (Table 1). Given that pathology in PPA is highly asymmetric—with language being the most salient clinical feature, and atrophy being often greater in the language-dominant hemisphere (33) and TDP-43 inclusions asymmetrically favoring language regions (30, 33)—we anticipated that an asymmetric distribution of TDP-43 pathology is possible in a way that would be distinct from the bvFTD cases. However, our counts of mature and preinclusions in the brains of PPA participants were not significantly different across hemispheres. Not surprisingly, the bvFTD brains also lacked significant asymmetry. Consistent with the well-known clinical preservation of memory function in PPA (33), our findings indicate that the hippocampus is not vulnerable to asymmetric pathologic deposition in the same manner as anatomic regions that are associated with language function (32). In fact, neither bvFTD nor PPA is characterized by the type of memory loss that is dependent on hippocampal function. Therefore, the hippocampal pathology we investigate in this study is either a late event in the course of the disease or is associated with a mechanism that protects the neurons from the toxic effects of TDP-43 inclusions.

It may be argued that the decreased density of mature TDP-43 inclusions in CA fields is due to neuronal degeneration and TDP-43 inclusions are being cleared / eliminated with dying neurons. However, this is an unlikely possibility given the preservation of memory in FTLD, and no reports of hippocampal degeneration in FTLD-TDP without concomitant hippocampal sclerosis. In fact, we have shown that cortical regions with greatest degeneration (highest atrophy), display highest densities of mature TDP inclusions (30, 32, 33). Moreover, we have not observed any discernible changes in the packing density of pyramidal neurons in the CA fields in the cases used in the current study. It may also be argued that the numbers of inclusions and preinclusions in our study is a function of the packing density of neurons in various hippocampal sectors, with the DG containing a higher density of neurons per volume than the CA fields. However, our findings cannot be explained based purely on the density of neurons. The DG in our study displayed substantial accumulation of inclusions and to a lesser extent preinclusions (Table 2). However, many CA sectors in a number of cases were completely devoid of inclusions. Moreover, despite lower packing density of neurons, CA3 contained substantially higher normalized counts of preinclusions as compared with the DG. It is possible that differential distribution of TDP-43 inclusions and preinclusions in CA fields and the DG granule cells are due to different vulnerability of neurons in these hippocampal sectors to formation of these abnormal precipitates rather than transsynaptic spread of pathology. However, this interpretation is unlikely given the differences seen in the numbers and densities of inclusions and preinclusions in different CA fields, which consist of relatively homogenous populations of pyramidal neurons with similar expected vulnerability.

Elucidating the possible mechanism of propagation of TDP-43 inclusions in FTLD is important, as FTLD-TDP not only comprises the largest proportion of FTLDs, but also can

lead to a perplexing heterogeneity of devastating clinical phenotypes. Our findings are significant not only in adding to the growing body of evidence that TDP-43 spreads through axonal pathways in a prion-like fashion but also in addressing the question of directionality of propagation, particularly in the human brain.

REFERENCES

1. Bahia V, Takada LT, Deramecourt V. Neuropathology of frontotemporal lobar degeneration: A review. Dement Neuropsychol 2013;7:19–26
2. Harvey R, Skelton-Robinson M, Rossor MN. The prevalence and causes of dementia in people under the age of 65 years. J Neurol Neurosurg Psychiat 2003;74:1206–9
3. Arai T, Hasegawa M, Akiyama H, et al. TDP-43 is a component of ubiquitin-positive tau-negative inclusions in frontotemporal lobar degeneration and amyotrophic lateral sclerosis. Biochem Biophys Res Commun 2006;351:602–11
4. Kwong L, Neumann M, Sampathu DM, et al. TDP-43 proteinopathy: The neuropathology underlying major forms of sporadic and familial frontotemporal lobar degeneration and motor neuron disease. Acta Neuropathol 2007;114:63–70
5. Rascovsky K, Hodges HJ, Knopman D, et al. Sensitivity of revised diagnostic criteria for the behavioural variant of frontotemporal dementia. Brain Res 2011;134:2456–77
6. Gorno-Tempini ML, Hillis AE, Weintraub S, et al. Classification of primary progressive aphasia and its variants. Neurology 2011;76:1006–14
7. Swinnen B, Robberecht W. The phenotypic variability of amyotrophic lateral sclerosis. Nat Rev Neurol 2014;10:661–70
8. Borroni B, Cosseddu M, Pilotto A, et al. Early stage of behavioral variant frontotemporal dementia: Clinical and neuroimaging correlates. Neurobiol Aging 2015;36:3108–15
9. Lanata S, Miller BL. The behavioural variant frontotemporal dementia (bvFTD) syndrome in psychiatry. J Neurol Neurosurg Psychiatry 2016; 87:501–11
10. Mesulam M. Primary progressive aphasia: A dementia of the language network. Dement Neuropsychol 2013;7:2–9
11. Neumann M, Sampathu DM, Kwong LK, et al. Ubiquitinated TDP-43 in frontotemporal lobar degeneration and amyotrophic lateral sclerosis. Science 2006;314:130–3.
12. Cairns NJ, Bigio EH, Mackenzie IR, et al. Neuropathologic diagnostic and nosologic criteria for frontotemporal lobar degeneration: Consensus of the Consortium for Frontotemporal Lobar Degeneration. Acta Neuropathol 2007;114:5–22
13. Aguzzi A, Falsig J. Prion propagation, toxicity and degradation. Nat Neurosci 2012;15:936–9
14. de Calignon A, Polydoro M, Suarez-Calvet M, et al. Propagation of tau pathology in a model of early Alzheimer's disease. Neuron 2012;73:685–97
15. Liu L, Drouet V, Wu JW, et al. Trans-synaptic spread of tau pathology in vivo. PLoS One 2012;7:e31302
16. Luk K, Kehm V, Carroll J, et al. Pathological alpha-synuclein transmission initiates Parkinson-like neurodegeneration in nontransgenic mice. Science 2012;338:949–53
17. Smethurst P, Sidle KC, Hardy J. Review: Prion-like mechanisms of transactive response DNA binding protein of 43κDa (TDP-43) in amyotrophic lateral sclerosis (ALS). Neuropathol Appl Neurobiol 2015;41:578–97.
18. Brettschneider J, Del Tredici K, Irwin DJ, et al. Sequential distribution of pTDP-43 pathology in behavioral variant frontotemporal dementia (bvFTD). Acta Neuropathol 2014;127:423–39
19. Lee E, Lee VM, Trojanowski JQ. Gains or losses: Molecular mechanisms of TDP43-mediated neurodegeneration. Nat Rev Neurosci 2012;13: 38–50
20. Udan M, Baloh RH. Implications of the prion-related Q/N domains in TDP-43 and FUS. Prion 2011;5:1–5
21. King OD, Gitler AD, Shorter J. The tip of the iceberg: RNA-binding proteins with prion-like domains in neurodegenerative disease. Brain Res 2012;1462:61–80
22. Furukawa Y, Kaneko K, Watanabe S, et al. A seeding reaction recapitulates intracellular formation of Sarkosyl-insoluble transactivation response element (TAR) DNA-binding protein-43 inclusions. J Biol Chem 2011;286:18664–72
23. Feiler MS, Strobel B, Freischmidt A, et al. TDP-43 is intercellularly transmitted across axon terminals. J Cell Biol 2015;211:897–911
24. Rosene D, Van Hoesen W. The hippocampal formation for the primate brain. A review of some camparative aspects of cytoarchitecture and connections. In: Cerebral Cortex. New York: Plenum Publishing 1987: 345–456
25. Armstrong RA, Carter D, Cairns NJ. A quantitative study of the neuropathology of 32 sporadic and familial cases of frontotemporal lobar degeneration with TDP-43 proteinopathy (FTLD-TDP). Neuropathol Appl Neurobiol 2012;38:25–38
26. Mackenzie IR, Baborie A, Pickering-Brown S, et al. Heterogeneity of ubiquitin pathology in frontotemporal lobar degeneration: Classification and relation to clinical phenotype. Acta Neuropathol 2006;112: 539–49
27. Kim G, Bolbolan K, Shahidehpour R, et al. Morphology and distribution of TDP-43 pre-inclusions in primary progressive aphasia. J Neuropathol Exp Neurol 2019;78:229–37
28. Mori F, Tanji K, Zhang HX, et al. Maturation process of TDP-43-positive neuronal cytoplasmic inclusions in amyotrophic lateral sclerosis with and without dementia. Acta Neuropathol 2008;116: 193–203
29. Geula C, Mesulam MM, Saroff DM, et al. Relationship between plaques, tangles, and loss of cortical cholinergic fibers in Alzheimer disease. J Neuropathol Exp Neurol 1998;57:63–75
30. Kim G, Vahedi S, Gefen T, et al. Asymmetric TDP pathology in primary progressive aphasia with right hemisphere language dominance. Neurology 2018;90:e396–e403
31. Geula C, Bu J, Nagykery N, et al. Loss of calbindin-D28k from aging human cholinergic basal forebrain: Relation to neuronal loss. J Comp Neurol 2003;455:249–59
32. Kim G, Bolbolan K, Gefen T, et al. Atrophy and microglial distribution in primary progressive aphasia with transactive response DNA-binding protein-43 kDa. Ann Neurol 2018;83:1096–104
33. Kim G, Ahmadian SS, Peterson M, et al. Asymmetric pathology in primary progressive aphasia with progranulin mutations and TDP inclusions. Neurology 2016;86:627–36
34. Mesulam M. Slowly progressive aphasia without generalized dementia. Ann Neurol 1982;11:592–8